A.4. Study of Molecular Systems

A.4.1. Ground State Dissociation of HD^+--*E. Wells, K.D. Carnes, B.D. Esry, O.L. Weaver, and I. Ben-Itzhak*

Vertical single ionization of hydrogen molecules leads predominantly to the creation of vibrationally bound molecular ions. A small percentage of the transitions, however, may end in the vibrational continuum of the electronic ground state, resulting in the dissociation of the transient molecular ion. For the heteronuclear HD^+ molecular ion, the dissociation can lead to two final states: $H^+ + D(1s)$ or $H(1s) + D^+$. The two final states correspond to the $1s\sigma$ and $2p\sigma$ potential energy curves of HD^+, respectively. These curves are not degenerate at the separate atom limit, as with H_2^+ or D_2^+, but are separated by 3.7 meV. Examination of this "ground state dissociation" (GSD) process, illustrated schematically in Fig. 1, has been a central part of our recent research. This project was the subject of Eric Wells' Ph.D. dissertation [1].

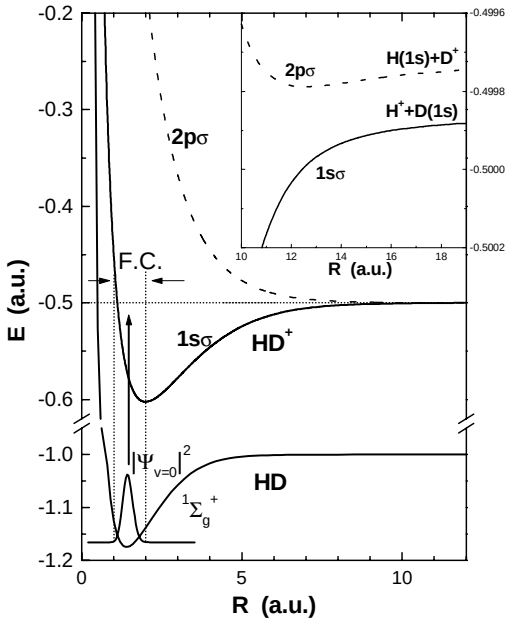

Figure 1. The potential energy curves for HD $^1\Sigma_g^+$ [2] and the two lowest electronic states of HD^+, $1s\sigma$ and $2p\sigma$ [3]. The energy gap between the $1s\sigma$ and $2p\sigma$ final states at the separate atom limit is 3.7 meV. In the GSD process, a fast projectile ionizes one electron of the neutral HD molecule, making a vertical (or Franck-Condon) transition to the HD^+ electronic ground state. If the result of the vertical ionization is a HD^+ molecular ion in the vibrational continuum, the molecule will dissociate into a H^+ ion and a D(1*s*) atom. A charge transfer reaction may take place near the avoided crossing at about R = 12 a.u., shown in the inset. If a charge transfer occurs, the final state will be $H(1s) + D^+$.

The HD^+ system provides a benchmark system for calculations of adiabatic potential energy curves by techniques extending beyond the Born-Oppenheimer approximation [3-6]. Scattering calculations of the associated low energy $H^+ + D(1s)$ or $D^+ + H(1s)$ collisions have also been conducted for some time [7-9], and there has been renewed interest recently [10], [Publication #103]. This charge transfer reaction is of applied interest in, for example,

astrophysical chemistry [11,12], since it is a main step in creating several deuterated molecules, notably HD. Several calculations for $H^+ + D(1s) \rightarrow H(1s) + D^+$ charge transfer, and the best available experimental data, are shown in Fig. 2. The experimental data of Newman *et al.* [13] clearly does not have sufficient resolution to probe theory, illustrating the difficulties in conducting traditional merged-beams experiments in this low energy range.

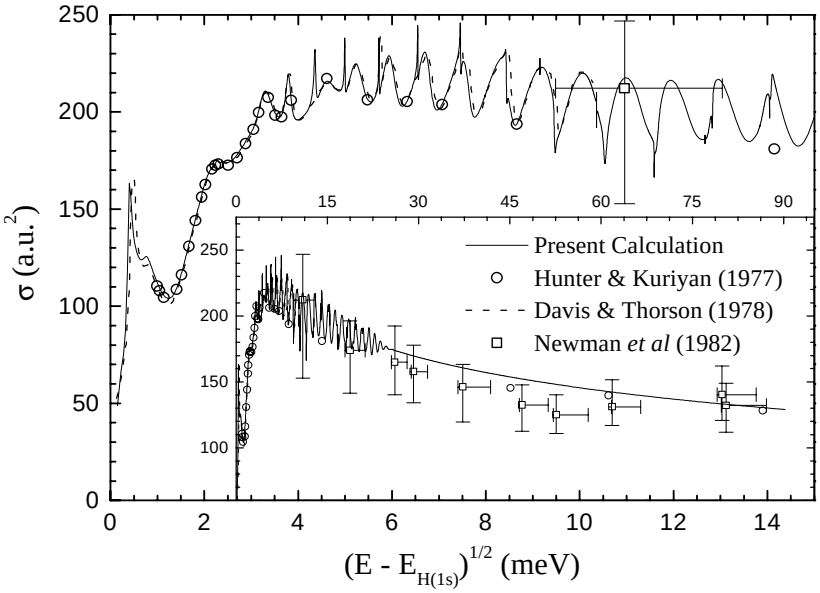

Figure 2. Comparison of calculations and experiment for the $H^+ + D(1s) \rightarrow H(1s) + D^+$ charge transfer reaction. The older calculations are from references [7] and [8] while the present calculation is from [10]. The measured values of Newman *et al.* are from reference [13].

The GSD process, however, opens an experimental window into this previously inaccessible energy region [Publication #62]. We use fast proton impact to "pump" the neutral HD molecule into the vibrational continuum of $HD^+(1s\sigma)$. Protons are chosen over more highly charged projectiles to reduce the number of higher energy H^+ and D^+ fragments from competing processes [Publication #83]. Since the single ionization of HD that is used to produce the HD^+ molecular ions happens on a time scale much shorter than the vibrational motion of the molecule, the initial and final states may be linked by the Franck-Condon factors. These calculations [14,15, Publication #15] show that about 1% of the vertical single ionization events reach the vibrational continuum and dissociate. The kinetic energy release (E_k) upon dissociation is typically quite small, peaking at E_k = 0 and with a width of approximately 300 meV. The dissociation process, which starts from a well defined initial state, $HD^+(1s\sigma)$ associated with the

H^+ + D(1*s*) limit, can be thought of as a "half" collision, since it starts from some finite internuclear distance and continues to R = ∞, as opposed to a typical "full" collision, which starts and ends at R = ∞. Furthermore, the range of kinetic energy release in these GSD events coincides with the energy region where merged-beams experiments become prohibitively difficult to perform.

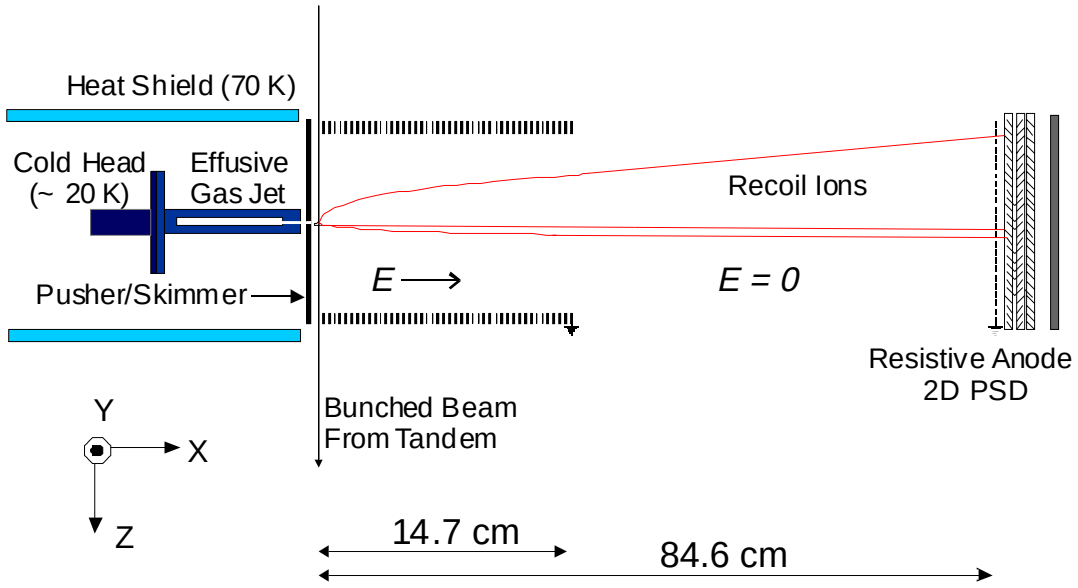

Figure 3. Conceptual view of our COLTRIMS-style momentum-imaging apparatus.

We study the GSD process by imaging the three dimensional momentum vector of the charged fragments produced in the dissociation. Our experimental technique has many features in common with COLTRIMS. A schematic view of our apparatus is shown in Fig. 3. We use a pre-cooled effusive jet to provide a cold localized target that is crossed by a bunched beam of fast protons. A weak extraction field is used to direct the charged fragments to a two-dimensional position sensitive detector. The non-uniform extraction field also forms a weak electrostatic lens, to focus the recoil ions in such a way as to compensate for extended target size, a common COLTRIMS technique [Publications #58 and #88]. By lowering the extraction field, we can spread the lowest energy GSD fragments over the entire face of the detector, and thus probe the GSD events near threshold with the highest resolution. P_x is evaluated from the fragment's time-of-flight, measured relative to a signal synchronized with the beam bunch. The details of this experimental technique can be found in Ref. [1,15].

Our measurements can be broken into two parts. We have measured the probability for charge transfer and elastic scattering as a function of E_k, as discussed later. Our first experimental step, however, was to demonstrate that there was a measurable asymmetry in the branching ratio of GSD of HD^+. Some hints of an asymmetry can be found in the work of Carrington *et al.*, who studied the HD^+ molecular ion using microwave spectroscopy [16]. They found that their spectroscopic measurements agreed with *ab initio* structure calculations only if corrections to the Born-Oppenheimer approximation were included. Furthermore, using the hyperfine multiplet splitting as a measuring tool, they found a strong asymmetry in the electron distribution for the v = 21 and v = 22 states (1.26 and 0.053 meV below the dissociation threshold, respectively), with the electron being located preferentially near the deuteron. An analogous situation in the vibrational continuum would mean that the 3.7 meV lower H^+ + D(1s) final state would be preferred over the higher H(1s) + D^+ final state. Since the energy gap between these two final states is so small compared to the range of kinetic energy released in the GSD process, it was questionable if an asymmetric branching ratio could be observed, especially when one considers that Carrington *et al.* [16] found the electron distribution of HD^+ to be essentially symmetric for the v = 18 state, 74.156 meV below threshold.

We have measured the branching ratio of H^+ + D(*1s*) to H(*1s*) + D^+ for GSD by measuring the relative yields of the H^+ and D^+ fragments produced in GSD. Any measurement of this GSD branching ratio is complicated by the inherent presence of H_2 and D_2 contaminants in the HD target. Since the resulting H_2^+ molecular ions have the same mass to charge ratio (m/q) as the D^+ GSD fragments of interest in this study, they overlap in the time-of-flight spectra, as shown in Fig. 4. We have developed two ways of measuring this contamination. The first (see Publication #15) uses the time-of-flight information in conjunction with the theoretical knowledge, derived from the Franck-Condon factors, of the bound-free to bound-bound ratios for H_2, HD, and D_2. The second method [1,15, Accepted #2] measures the H_2^+ yield directly using the two-dimensional momentum distribution of the HD^+ molecular ion as a high statistics simulation of the H_2^+ contamination in the m/q = 2 momentum distribution. This process is illustrated in Fig. 4. The two methods yield consistent results. The results of our measurements of the branching ratio, summarized in Table I, show that the H^+ + D(1s) channel is the favored one, independent of the technique used to determine the H_2^+ contamination. The difference in the relative yield of the two dissociation channels, while small, is significant (2.1σ) indicating a

measurable symmetry breakdown in the GSD of HD^+. This empirically demonstrates, for the first time, that the isotopic effect leading to the breakdown of the Born-Oppenheimer approximation for HD^+ causes not only small changes of the potential energy curves and localization of the electron density on the deuteron for highly excited vibrational states, but also is responsible for the measurable preference of D(1*s*) over H(1*s*) in the dissociation of the molecular ion. Stated another way, the localization of the electron density on the deuteron occurs not only for vibrationally bound states, but also in the vibrational continuum. This result has recently been accepted for publication in Physical Review Letters [Accepted #2].

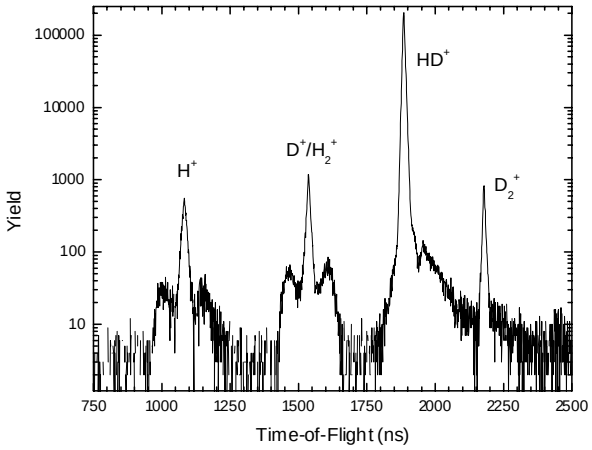

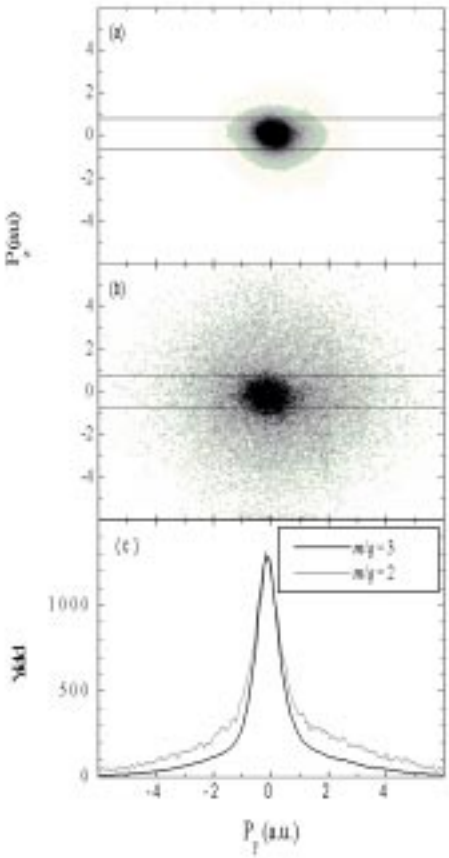

Figure 4. **Above:** A typical time-of-flight spectrum showing the H_2^+ and D_2^+ contaminations. Note that the H_2^+ contamination overlaps the D^+ fragments. **Right:** (a) Momentum distribution for HD^+ ion. (b) Momentum distribution for the combination of H_2^+ molecular ions and D^+ GSD fragments. In both (a) and (b) the same shades of gray represent the same percentage of the maximum. (c) Slices of (a) and (b) where the m/q = 3 slice has been scaled to have the same amplitude as the m/q = 2 slice. The scaling factor needed to make the amplitudes match represents the H_2 contamination level.

We have treated this problem theoretically by calculating the $1s\sigma$ to $2p\sigma$ transition probability, *w*, as a function of kinetic energy release using a coupled channels method [15, Accepted #2]. In addition, we have adapted the Meyerhof model [17] for K-shell vacancy sharing in near-symmetric ion-atom collisions to this problem. By convoluting $w(E_k)$ with the probability of a GSD event as a function of energy, $P(E_k)$, and integrating that result over the

entire range of E_k, a total charge transfer probability is obtained. These results are also summarized in Table I. Somewhat surprisingly, the Meyerhof model provides an accurate estimate even at these low collision velocities. There is, however, some ambiguity in the Meyerhof model with regard to the definition of the relative nuclear velocity. We have found that the Meyerhof formula works best if the velocity is defined relative to the D(1s) final state and the resulting probability is truncated in the region where charge transfer is energetically forbidden.

Method	**H^+ + D(1*s*) (%)**	**H(1*s*) + D^+ (%)**	**GSD (HD^+) (%)**
Time-of-flight	0.527 ± 0.011	-	-
Momentum Imaging[a]	0.525 ± 0.009	0.464 ± 0.021	0.989 ± 0.022
Momentum Imaging[b]	0.522 ± 0.012	0.478 ± 0.022	1.000 ± 0.025
Coupled Channels	0.539	0.455	0.994
Truncated Meyerhof KER = $E - E_{D(1s)}$	0.536	0.458	0.994

Table I. The results of our integrated measurements. The experimental results include the results obtained using only the time-of-flight measurement and measurements using momentum imaging to determine the H_2 contamination with 4 MeV Proton Projectiles[a], and with 20 MeV C^{3+} Projectiles[b]. These results are compared to calculated values obtained with coupled channels calculations and the Meyerhof model. In the Meyerhof calculation, computation of the Franck-Condon overlap integrals gives the total GSD fraction for HD^+, and the Meyerhof model is used to obtain the branching ratio.

While the integrated measurements presented above show that there is a measurable preference for the electron to be associated with the deuteron, a much more interesting measurement would be to probe this preference as a function of kinetic energy release. In other words, the quantity to be measured is the transition probability, $w(E_k)$, between the lower $1s\sigma$

and the upper $2p\sigma$ states. In addition, since the detection of a H^+ fragment indicates that there was no transition to the $2p\sigma$ state, the probability for elastic scattering in H^+ + D(1*s*) half collisions can also be measured as a function of kinetic energy release. The ability to probe the transition probabilities experimentally rests on the precise measurement of the momentum of the dissociating fragments in the center of mass frame. By cooling our HD target to approximately 15 K, using a very weak extraction field, and carefully working to improve the resolution of the time-of-flight and position measurements, we are currently able to measure the energy of the dissociating GSD fragments with a resolution of approximately 2-3 meV for the lowest extraction fields used. This resolution is sufficient to probe the charge transfer and elastic scattering processes in H^+ + D(1*s*) "half" collisions at collision energies an order of magnitude lower than possible with conventional merged-beams approaches. Our measurements of $w(E_k)$ are shown in Fig. 5, along with the theoretical predictions from our coupled channels calculations and the Meyerhof model. Near threshold, there is a systematic experimental error related to our inability to precisely subtract the H_2 contamination (in a differential manner) due to isotopic effects in the velocity distribution of the effusive jet [1]. Away from threshold, however, there is good agreement between theory and experiment.

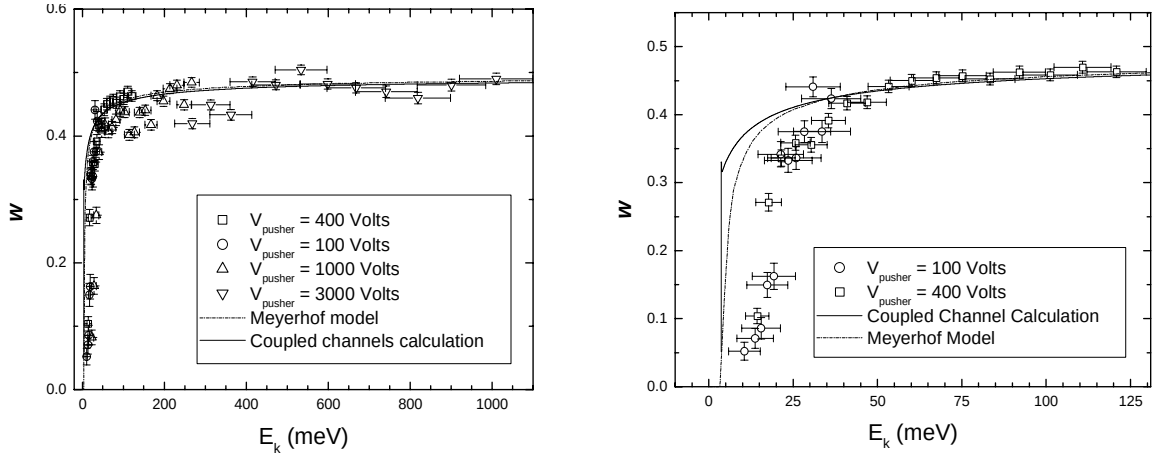

Figure 5. The measured transition probability, *w*, as a function of E_k. The results are compared to the coupled channels calculations and the Meyerhof model. **Left:** Results from 4 different extraction voltages are combined to cover the entire energy range of GSD events. **Right:** An expanded view of the data near threshold. The systematic error in the H_2 subtraction is clear in this figure, with the threshold for a transition appearing to be at about 13 meV, rather than the 3.7 meV predicted by theory. In the region above $E_k \approx 50$ meV, where the H_2 contamination plays only a small role, the agreement between theory and experiment is quite good.

The elastic channel is particularly interesting just below the H(1*s*) threshold, where two Feshbach resonances are located for $l = 0$, effectively the only rotational state populated at the temperature (~15 K) of our target. Our results for the elastic channel are shown in Fig. 6. So far, we lack the momentum resolution to probe the resonance structure. For higher values of E_k, our experimental and theoretical results are once again in good agreement. This channel is an interesting candidate for future studies, since improvements in the momentum resolution of our apparatus should allow the general features of the resonance structure to be measured. Converting our apparatus to be ultra-high vacuum compatible will reduce the background from water vapor in the target, essentially eliminating the major competing channel. The elastic channel has two inherent advantages over the charge transfer channel with regards to resolution. First, the H_2 contamination is of much less importance in this channel. Second, the multiplicative factor needed to convert from lab to center-of-mass energy for the measured H^+ fragments is half that of the D^+ fragments.

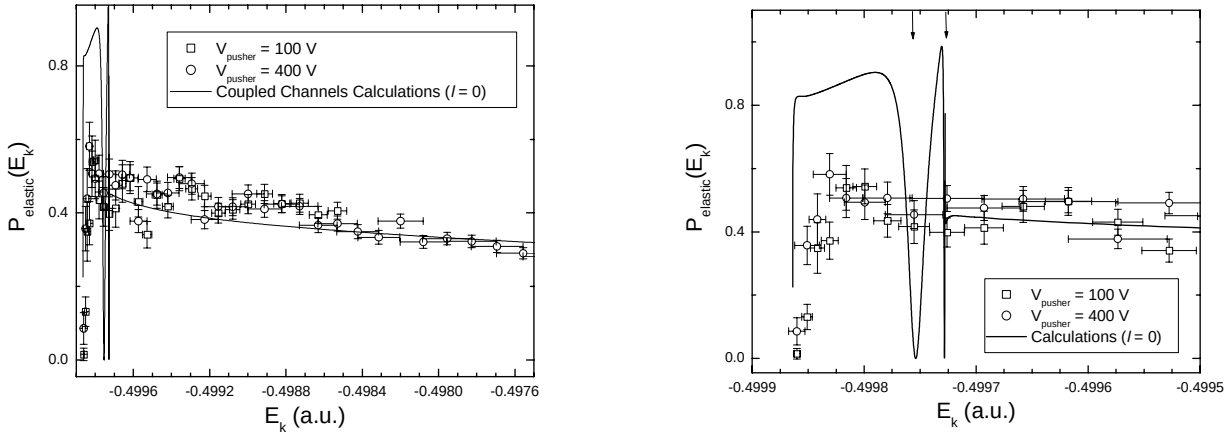

Figure 6. Left: The measured and calculated probabilities for elastic scattering measured in this experiment. The calculated value is for $l = 0$ only, which to a very good approximation, is the only state populated in our measurement, since the temperature of the target is approximately 15 K. **Right:** The measured and calculated probabilities for elastic scattering in the region of the H(1s) threshold. The arrows point out the locations of the two $l = 0$ Freshbach resonances just below the H(1s) threshold.

This project has been the subject of invited talks at the 1998 DAMOP meeting [Abstract #6], 1999 ISIAC conference [Abstract #97], and will be the subject of an invited talk by former graduate student Eric Wells at the CAARI 2000 conference in November.

References

1. E. Wells, Ph.D., Thesis, Kansas State University, unpublished, (2000).
2. W. Kołos, K. Szalewicz, and H.J. Monkhorst, J. Chem. Phys. 84, 3278 (1986).
3. B.D. Esry and H.R. Sadeghpour, Phys. Rev. A 60, 3604 (1999).
4. J. Macek, and K. A. Jerjian, Phys. Rev. A 33, 233 (1986).
5. M.C. Struensee, J.S. Cohen, and R.T. Pack, Phys. Rev. A 34, 3605 (1986).
6. R.E. Moss, J. Phys. B 32, L89 (1999).
7. G. Hunter and M. Kuriyan, Proc. R. Soc. Lond. A 358, 321 (1977).
8. J. Davis and W.R. Thorson, Can. J. Phys. 56, 996, (1978).
9. R.R. Hodges, Jr., Journal of Geophysical Research 98, 10833 (1993).
10. B.D. Esry, H.R. Sadeghpour, E. Wells, and I. Ben-Itzhak, to be submitted to J. Phys. B (2000).
11. P.C. Stancil, S. Lepp, and A. Dalgarno, The Astrophysical Journal 509, 1 (1998).
12. D. Galli and F. Palla, Astron. Astrophys. 335, 403 (1998).
13. J.H. Newman, J.D. Cogan, D.L. Zeigler, D.E. Nitz, R.D Rundel, K.A. Smith, and R.F. Stebbings, Phys. Rev. A 25, 2976 (1982).
14. I. Ben-Itzhak, Vidhya Krishnamurthi, K.D. Carnes, H. Aliabadi, H. Knudsen, U. Mikkelsen, and B.D. Esry, J. Phys. B 29, L21 (1996).
15. E. Wells, B.D. Esry, K.D. Carnes, and I. Ben-Itzhak, to be submitted to Phys. Rev. A. (2000).
16. A. Carrington, Science, 274, 1327 (1996); A. Carrington, I.R. McNab, C.A. Montgomerie-Leach, and R.A. Kennedy, Mol. Phys. 72, 735 (1991), and references therein.
17. W.E. Meyerhof, Phys. Rev. Lett. 31, 1341 (1973).